FABRICATION AND PERFORMANCE TESTING OF CaO INSULATOR COATINGS ON V-5%Cr-5%Ti IN LIQUID LITHIUM*

J.-H. Park and G. Dragel (Argonne National Laboratory)

OBJECTIVE

Corrosion resistance of structural materials, and the magnetohydrodynamic (MHD) force and its influence on thermal hydraulics and corrosion, are major concerns in the design of liquid–metal blankets for magnetic fusion reactors (MFRs). The objective of this study is to develop in–situ stable coatings at the liquid-metal/structural-material interface, with emphasis on coatings that can be converted to an electrically insulating film to prevent adverse currents that are generated by the MHD force from passing through the structural walls.[1,2]

SUMMARY

The electrical resistance of CaO coatings produced on V-5%Cr-5%Ti by exposure of the alloy to liquid Li that contained 0.5-85 wt.% dissolved Ca was measured as a function of time at temperatures between 250 and 600°C. The solute element, Ca in liquid Li, reacted with the alloy substrate at 400-420°C to produce a CaO coating. Resistance of the coating layer measured in-situ in liquid Li was ≈0.4 and $6.4 \times 10^6\ \Omega$ at 267 and 400°C, respectively. Thermal cycling between 300 and 700°C changed the resistance of the coating layer, which followed insulator behavior. Examination of the specimen after cooling to room temperature revealed cracks in the CaO coating; therefore preliminary tests were conducted to investigate in-situ self-healing behavior. At ≥360°C, relatively fast healing was indicated. These results suggest that thin homogeneous coatings can be produced on variously shaped surfaces by controlling the exposure time, temperature, and composition of the liquid metal. This coating method is applicable to reactor components. The liquid metal can be used over and over because only the solutes are consumed, not the liquid metal itself. The technique can be applied to various shapes (e.g., inside/outside of tubes, complex geometrical shapes) because the coating is formed by liquid-phase reaction.

INTRODUCTION

Corrosion resistance of structural materials, and the MHD force and its influence on thermal hydraulics, are major concerns in the design of liquid–metal cooling systems for fusion first–wall/blanket applications.[1] Vanadium and V-base alloys (V-Ti or V-Ti-Cr) are leading candidate materials for structural applications in fusion reactors.[3] Previous studies focused on in-situ formation of AlN in liquid Li on an aluminide substrate on V-5Cr-5Ti produced by a chemical vapor deposition method.[4,5] Our recent work has focused on in-situ formation of CaO on V-5Cr-5Ti in liquid Li because the electrical resistivity of CaO is greater than that of AlN by a factor of 10,000 (Fig. 1), and because CaO exhibits a higher thermodynamic stability (Fig. 2) than that of other potential insulator candidates (BeO, MgO, $MgAl_2O_4$, $Y_3Al_2O_{12}$, etc.) in liquid Li.[6,7] The objective of this study is to develop in-situ corrosion–resistant coatings, as well as electrically insulating coatings at the liquid-metal/structural-material interface. These coatings should be capable of forming on various shapes such as the inside of tubes or irregular shapes to prevent adverse currents that are generated by MHD forces from passing through the structural walls. The coatings could also improve general corrosion resistance and act as a diffusion barrier for hydrogen isotopes, viz., deuterium and tritium.

---

*This work has been supported by the U.S. Department of Energy, Office of Fusion Energy Research, under Contract W-31-109-Eng-38.

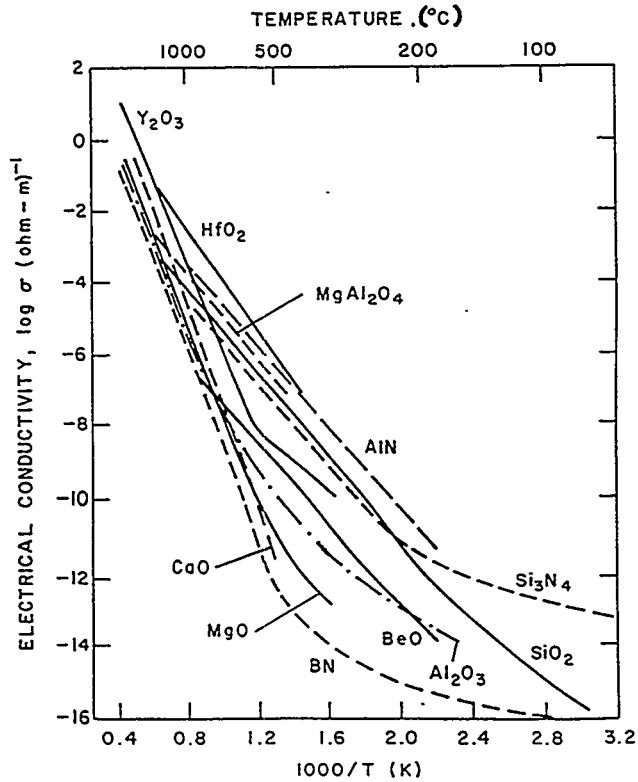

Figure 1. Electrical conductivity of candidate oxide and nitride insulators

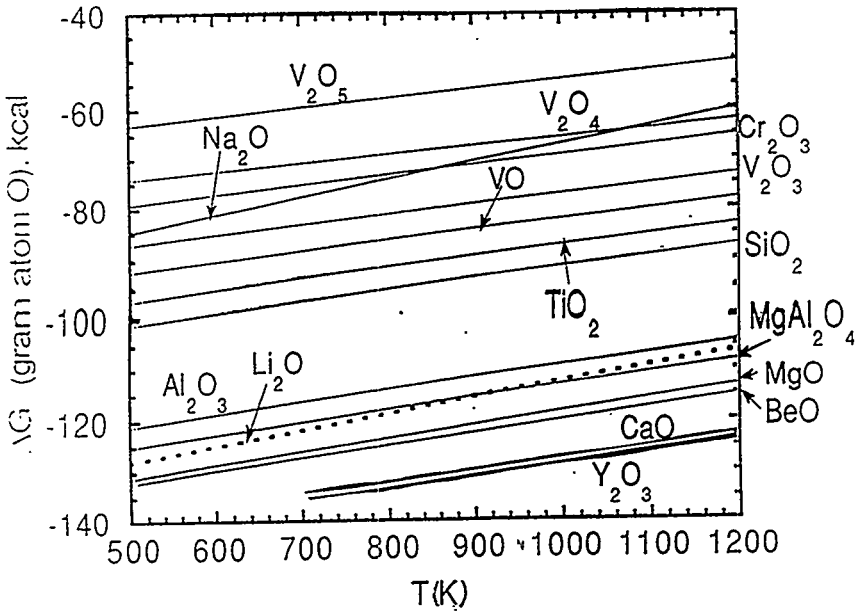

Figure 2. Free energy of formation of various oxides

EXPERIMENTAL PROCEDURE

Various experimental methods have been explored to fabricate and characterize insulator coatings for use in liquid–Li environments: (a) oxygen (O) charging of the near–surface region of V–base alloys in Ar gas and in air, (b) evaluation of liquid-Li compatibility of the O–charged specimens, (c) reaction of the O–enriched V–base alloy with dissolved Ca in Li to form the CaO layer, (d) in-situ electrical resistance measurements of CaO coatings on V-5Cr-5Ti in liquid Li, (e) characterization of the O–charged specimens and insulator coatings by microhardness measurements and scanning electron microscopy (SEM), and (f) optical examination of the coatings for evidence of surface defects such as spallation or cracks. Thermal cycling tests were also conducted to investigate the integrity of coating layers that formed in–situ. Fabrication of coatings at a relatively low temperature (≈400°C) has been emphasized so that the methods can be readily adapted to ITER components.

Oxygen charging of the surface of V-5Cr-5Ti

Metallic solutes dissolved in Li (e.g., Ca, Y, or Mg) do not produce intermetallic phases on V–base alloys, nor do they become incorporated into the material by diffusion interactions at low temperatures. Consequently, another approach was adapted to facilitate formation of an insulating coating (CaO): O was charged into the near–surface region of the alloy under controlled conditions. It is well known that O can be incorporated into the interstitial sublattice in body-centered-cubic (bcc) V and its alloys.[8] Thus, if O or N is present in the alloy (as a reactant), these elements may have a higher affinity for solutes, such as Ca, Y, or Mg dissolved in Li, compared to that of the alloy elements. In the bcc lattice of V-5Cr-5Ti, O can occupy interstitial sites within the lattice up to several atomic percent. Oxygen charging of V-5Cr-5Ti was conducted for up to 48 h at temperatures between 500 and 1030°C in flowing high–purity Ar and N_2 (99.999%) that contained O as an impurity. Specimen weight gain vs. reciprocal temperature is shown in Fig. 3. Diffusion coefficients of O and N in V (Fig. 4) show that diffusion of O in V is 10 to 1800 times faster than that of N. This property is very important for in-situ formation of CaO. Oxygen charging in an N_2 atmosphere lowers the rate (≈5%) because of some participation of N compared with an Ar atmosphere. However, O incorporation into V-5Cr-5Ti predominates even in a 99.999% pure N_2 atmosphere.

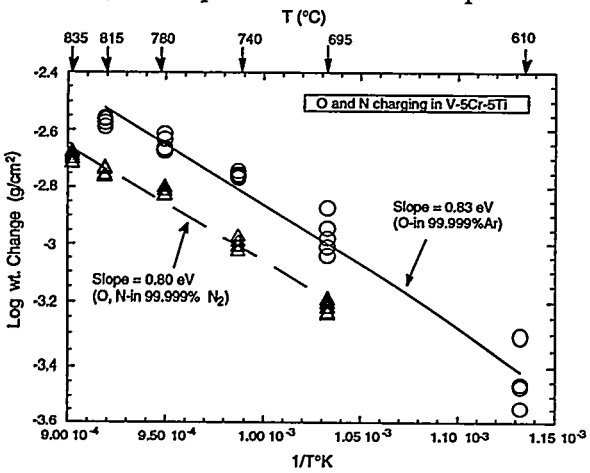

Figure 3. Weight gain of V-5Cr-5Ti vs. reciprocal temperature after exposure to flowing Ar and N_2 for 48 h

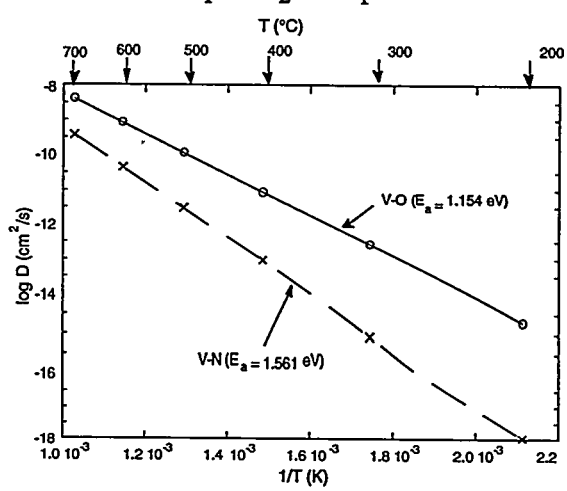

Figure 4. O and N diffusion in V calculated from data in R. Farraro and R. B. McLellan, Mat. Sci. and Eng., 39 (1979) 47-56

Figure 5(a) shows the weight gain per unit area of the alloy at various temperatures after 17 h in N_2, and Fig. 5 (b) shows a cross–sectional view of the specimens. The shiny area at the edge of the specimens depicts the region where O and N are incorporated into the interstitial sublattice of the V-5Cr-5Ti. Based

on visual observation and weight gain, we can control the depth of the O–charged layer by exposure temperature and time in a flowing Ar atmosphere. In this study, 99.999% Ar or N_2 was used for O charging. Figure 6 shows SEM photomicrographs of cross sections of V-5Cr-5Ti specimens that were charged with O by exposure to Ar at various temperatures. Oxygen enrichment along grain boundaries is more prevalent at higher temperatures. Oxygen concentration in the near–surface layer was calculated from the weight gain, surface area, and thickness of the hardened region. The O concentration ranged from 250 ppm (as–received) to ≈2–3%, depending on position within the layer and exposure conditions.

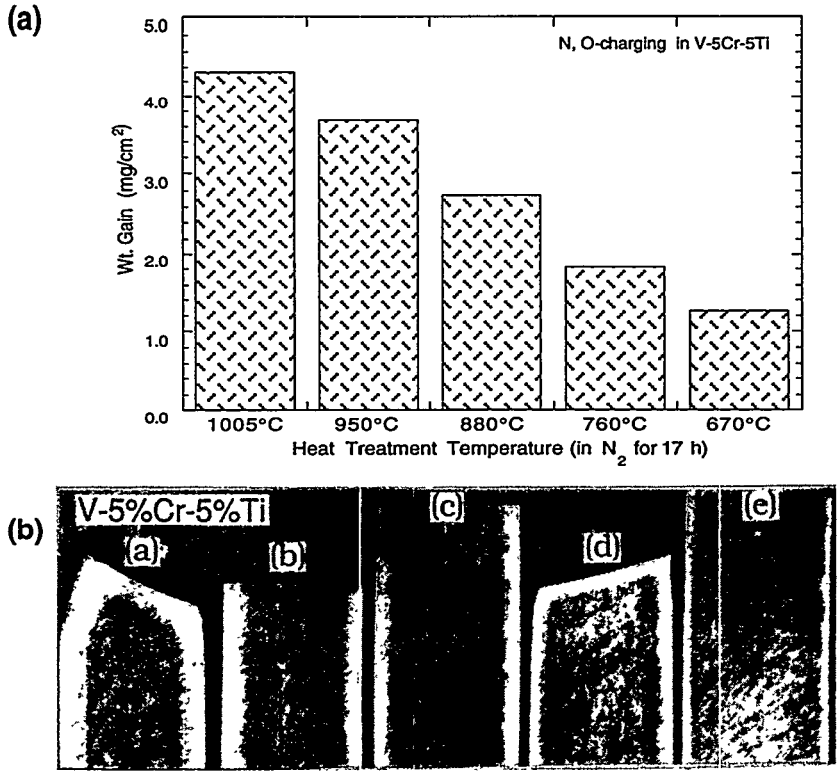

Figure 5. (a) Weight gain of V-5Cr-5Ti specimens after exposure in 99.999% N_2 for 17 h at several temperatures and (b) photomicrographs of specimen cross sections showing O–charged layer

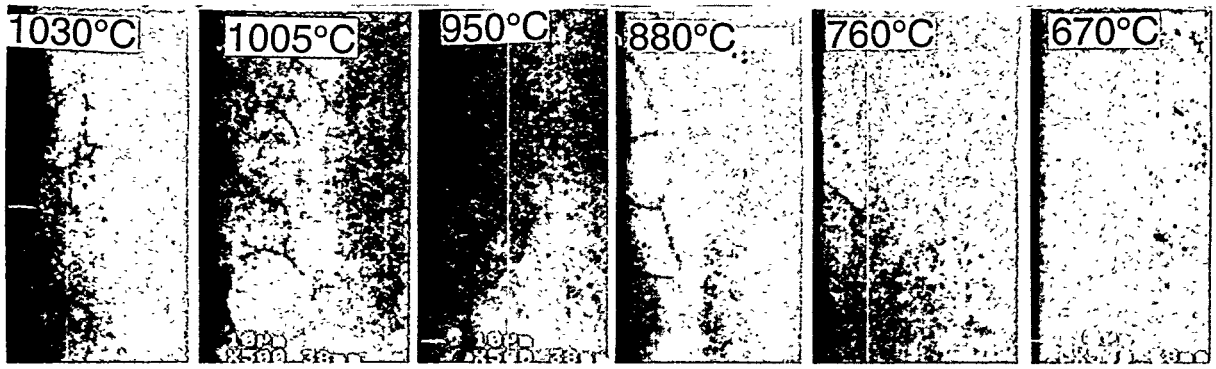

Figure 6. SEM back–scattered electron image from cross sections of V-5Cr-5Ti specimens showing O-charged near–surface region

Oxygen charging was also performed in air at 400°C to avoid melting of V_2O_5 (690°C) during oxidation. Figure 7 shows X-ray diffraction spectra from the surface region of specimens for two heat–treatment conditions. Figure 7(a) corresponds to oxidation in air at 400°C for 20 h, whereupon a blue amorphous layer (≈1 μm) formed at the surface, and Fig. 7(b) represents a similar layer formed by exposure of a V-5Cr-5Ti specimen to high–purity Ar at 650°C for 17 h. Samples charged with O in high–purity Ar or N_2 atmospheres showed the same X-ray spectra before and after O charging. When we measured the ohmic resistance (two–point contact) on the surfaces of heat–treated specimens at room temperature, the specimens charged with O in high–purity Ar or N_2 showed the same ohmic values before and after O charging. The blue oxide that formed in air at 400°C had a resistance of ≈5 Ω, not very high in comparison with values for most metal oxides. This oxide is not stable in liquid Li, as shown in Fig. 2.

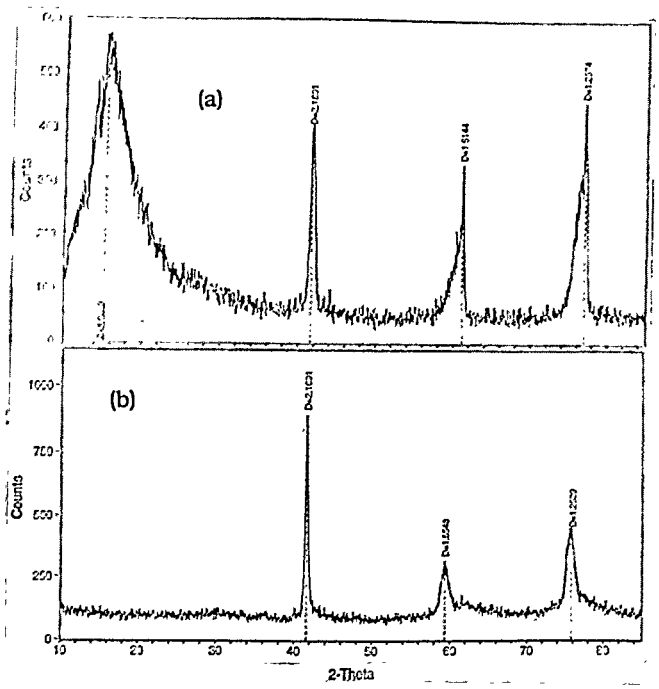

Figure 7.
X-ray diffraction spectra of V-5Cr-5Ti specimens (a) after oxidation in air for 20 h at 400°C, and (b) after O charging in Ar for 17 h at 650°C

Microhardness tests on O-charged V-alloys

Vickers hardness of the O–charged layers and the underlying V-5Cr-5Ti alloy was measured with a 50–g load. Figure 8 shows that the O–charged layers were much harder than the as–received alloys, which can be attributed to interstitial O atoms in the bcc lattice of V. The hardening mechanism appears to be somewhat different than that in most cases where precipitates form in the bulk alloy. Oxygen–charging experiments were performed on pure V, V-10Cr, and V-20Ti specimens in the same atmospheres as for V-5Cr-5Ti to obtain more insight into the hardening phenomenon. Pure V showed the highest hardness values among the different specimens, but the O–charged V-10Cr sample appeared to be more brittle during indentation. Figure 9 shows the dependence of room–temperature Vickers hardness of specimens on temperature of exposure (490 to 890°C) in high–purity Ar for 24 h. Transmission electron microscopy will be performed on several specimens to determine whether the hardening mechanism involves primarily occupation of interstitial sites by O or formation of small particles of V-O.

Compatibility tests on O-charged V-5Cr-5Ti in liquid Li

Figure 10 shows results of compatibility tests on O–charged samples in flowing liquid Li at 443°C for 298 h. Samples charged with O at 1030 and 1005°C showed the highest weight loss during exposure to liquid Li. Results for a similar test at 408°C for 239 h are shown in Fig. 11 for as–received specimens

(250 ppm O) and specimens that were charged with O under different time–temperature conditions. In general, specimens that exhibit the largest weight gain during O charging undergo the largest weight loss during exposure to Li. Presumably, this indicates that an oxide phase (e.g., V_2O_3) that formed during O-charging dissolves in liquid Li. However, weight–loss rates for specimens exposed to Li at 443 and 408°C are virtually the same (i.e., ≈0.0005 g/298 h/cm^2 or 1.68 μg/cm^2-h and ≈0.0002 g/239 h/cm^2 or 0.84 μg/cm^2-h, respectively). In contrast, if weight loss in short–term corrosion tests was controlled primarily by O diffusion in the alloy, the rates would be expected to be relatively independent of the amount of O charged. If O transport to liquid Li was controlled by diffusion in the alloy, diffusion data in Fig. 4 could be used to optimize time–temperature conditions for in-situ formation and self–healing of a CaO coating. This would be applicable to any of the thermodynamically stable oxides in the liquid Li, e.g., BeO, MgO, Y-Al-O garnet, Mg-Al-O spinel, Y_2O_3, and CaO etc., shown in Fig. 2. A similar situation could presumably occur for the formation of nitrides by the reaction of N in the alloy with metallic elements dissolved in Li.

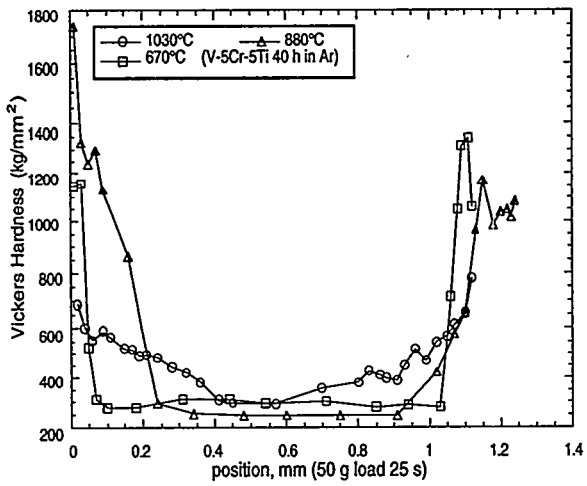

Figure 8. Vickers hardness profiles from cross sections of V-5Cr-5Ti specimens exposed to Ar for 40 h at 670, 880, and 1030°C

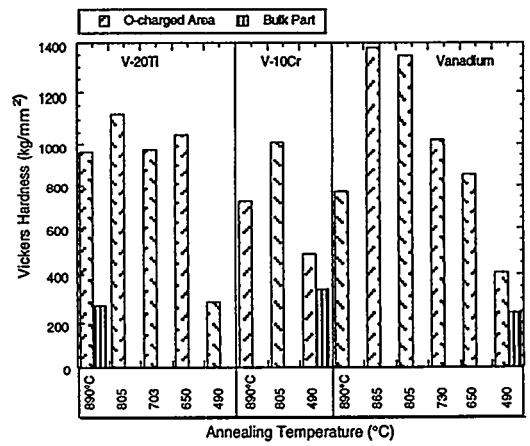

Figure 9. Vickers hardness from cross sections of V-20Ti, V-10Cr, and nonalloyed V specimens in near–surface and center regions after exposure in Ar for 24 h at several temperatures between 490 and 890°C

Nevertheless, it is important to determine the optimum condition for O-charging of V-5Cr-5Ti. Figure 12 shows photomicrographs of the cross sections of O–charged specimens (charging conditions analogous to those in Fig. 10) after exposure in flowing Li for 298 h at 443°C. The dark microstructural features in the near–surface region of the V-5Cr-5Ti specimens charged with O at ≥760°C are not confined to the O–enriched regions or the grain boundaries in the material. They seem to have developed via a phase transformation process during exposure to liquid Li. This phenomenon will be investigated in more detail in the future. Because the specimen charged with O at 670°C did not show these features, further O-charging was conducted at 650°C.

Vickers hardness of liquid–Li exposed specimens was measured with a 50–g load (Fig. 13). When we compare Vickers hardness of the cross section in the near–surface region (≈10 μm) of a specimen charged with O at 1030°C before and after liquid–Li exposure, we find that values were 600-700 and 1400-1600 kg/mm^2, respectively. This suggests that O diffused into the near–surface region. Oxygen charging at lower temperatures typically produces higher near–surface hardness values, as was shown in Fig. 8. Specimens charged with O at 880 and 670°C had relatively high near–surface hardness and hardness decreased after exposure to liquid Li.

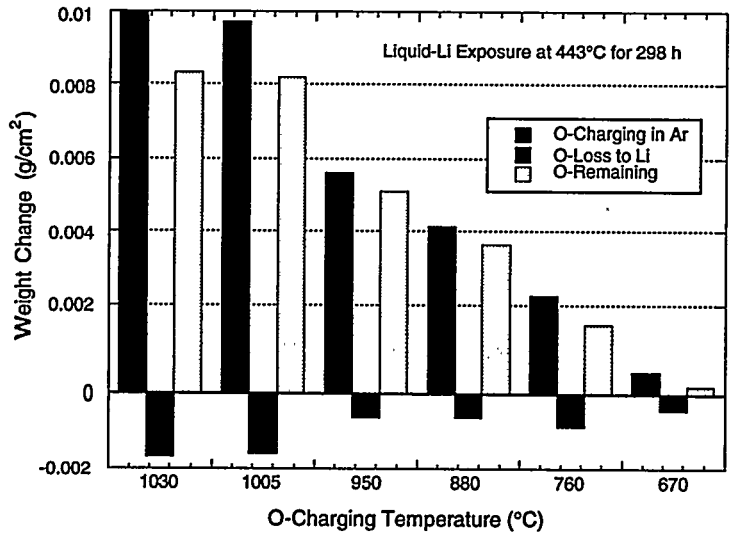

Figure 10.
Weight change of V-5Cr-5Ti specimens after O charging in Ar for 40 h at temperatures between 670 and 1030°C and after exposure of the O–charged specimens to Li at 443°C for 298 h

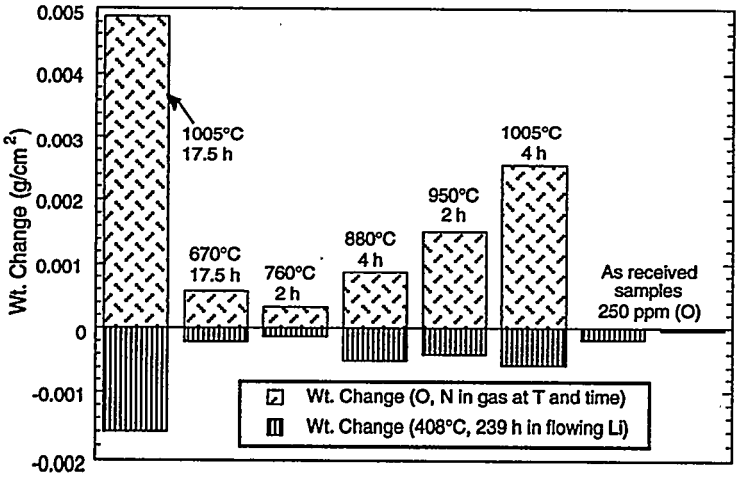

Figure 11.
Weight change of V-5Cr-5Ti specimens after O charging in N_2 at several temperatures between 670 and 1005°C for 2 to 17.5 h and after exposure of as–received and O–charged specimens to Li at 408°C for 239 h

CaO coating on V-5Cr-5Ti

CaO formation on as–received specimens: In-situ formation of CaO on as–received specimens (250 ppm O) has been investigated in liquid Li containing 4 at.% Ca in a Type 304 stainless steel capsule at 700°C during a 7–day exposure. Figure 14 shows an SEM photomicrograph and an EDS spectrum taken from the CaO surface layer. We believe the reaction to form CaO takes place at the interface between O at alloy surface and Ca in the liquid metal. The coating did not completely cover the V-5Cr-5Ti surface, but a high ohmic resistance typical of CaO (two–point contact of >20 MΩ at room temperature) was obtained.

CaO formation on O-charged specimens: To improve the formation of CaO on alloy substrates, O–charged specimens were immersed in Ca-bearing (0.5–85 wt.% Ca) liquid Li for various times and temperatures. This approach was adopted because O in the alloy (as a reactant) may have a higher affinity for a solute such as Ca dissolved in Li compared to that of the alloy elements (i.e., V, Cr, and Ti). Several experiments were performed to test this hypothesis. Specimens of V-5Cr-5Ti were heat–treated in flowing Ar at 650°C to charge the surface of the alloy with O. Because oxides of V are not stable in liquid Li (Fig. 2), conditions were controlled to avoid their formation on the surface during O charging.

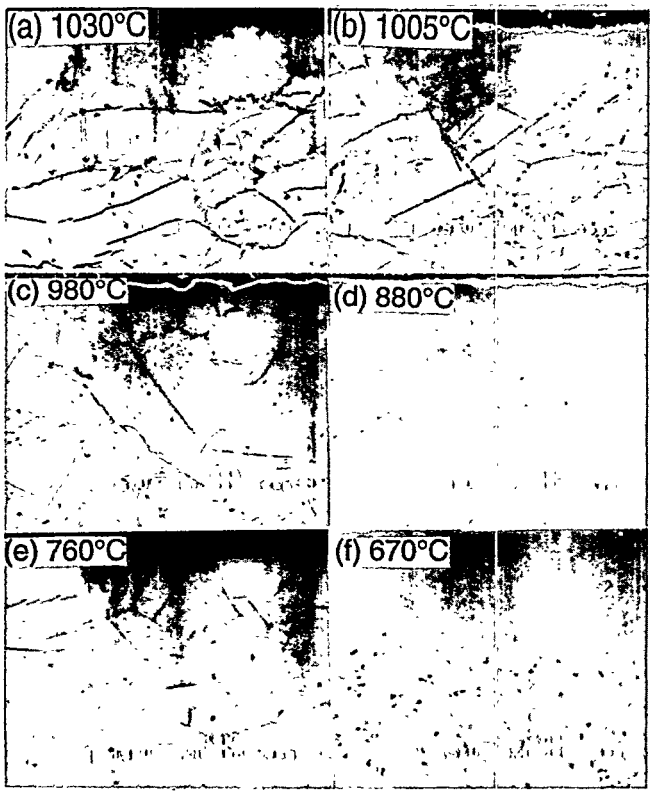

Figure 12.
Photomicrographs of cross sections in the near–surface region of O–charged V-5Cr-5Ti specimens after exposure to Li at 443°C for 239 h. Specimens were charged with O at several temperatures between 670 and 1030°C.

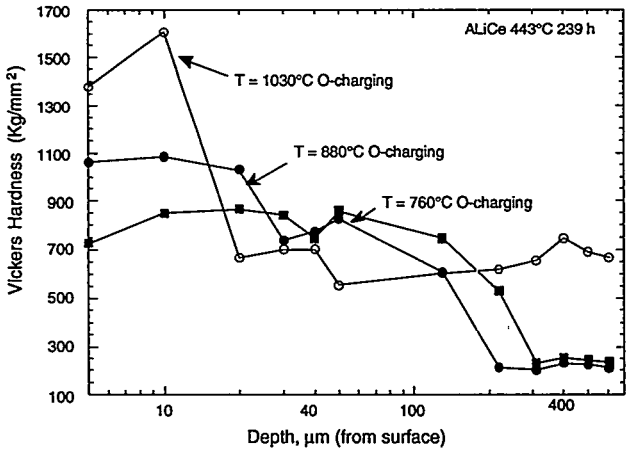

Figure 13.
Vickers hardness vs. depth for O-charged V-5Cr-5Ti specimens after exposure to Li at 443°C for 239 h

Our previous experiments focused on formation of CaO coatings on O-charged V-5Cr-5Ti at 416-750°C. Present results were obtained at 400°C, a temperature that is more consistent with ITER operating conditions. To monitor coating development by electrical resistivity measurements, specimens (1/4" x 1-1/2" x 0.04") were attached to Type 304 stainless steel lead wires (1.2 mm diameter) by electron–beam welding. The specimens were charged with O in an Ar atmosphere at 650°C for 17-20 h, as described previously. Figure 15 shows a set of four specimens after O charging. Two specimens were coupled to form one conductivity measuring unit, as described in a previous report.[4]

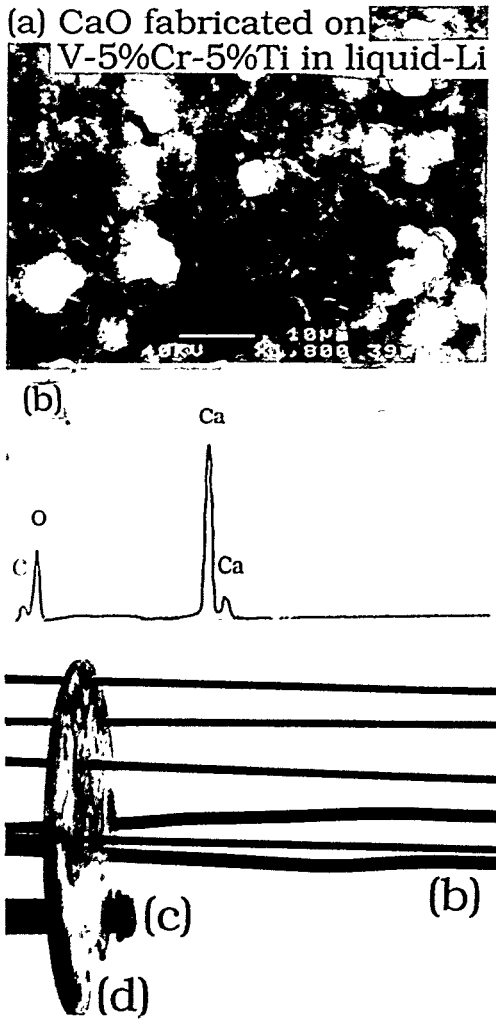

Figure 14.
(a) Photomicrograph of surface of CaO coating formed on as–received V-5Cr-5Ti (250 ppm O) at 700°C and (b) EDS of surface

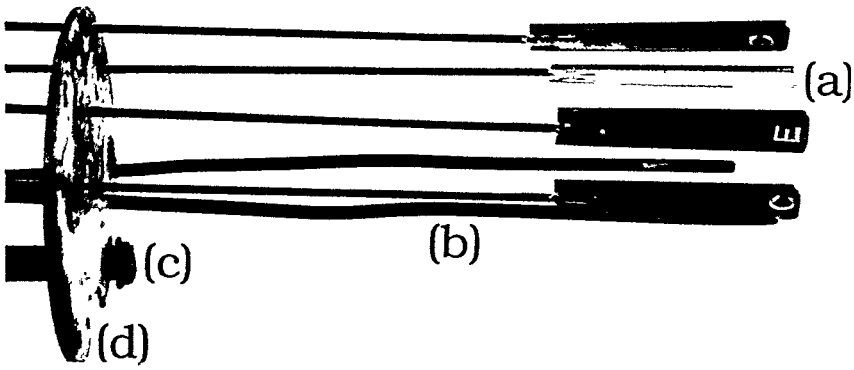

Figure 15. O-charging apparatus consisting of four V-5Cr-5Ti specimens welded to Type 304 stainless steel rods, (b) two K-type thermocouples, (c) Ar injection tube, and (d) spacer

The specimens were immersed for 17 h at 400°C in a solution of Li containing 85 wt.% of Ca, which has a liquidus temperature of ≈380°C. Then the specimens were raised above the liquid level and exposed to an Ar atmosphere at either 400°C or 650°C to oxidize the Ca, similar to the O-charging procedure for the V–base alloy. The specimens were immersed in the liquid Li-Ca alloy again to measure the electrical resistance of CaO films at 400°C. The temperature vs. time history is depicted in Fig. 16. The high resistance values exceeded the 20 MΩ range of the instrument. Only the open–circuit voltage (E_{oc}) of ± 2.336 could be measured with a digital voltmeter (DVM). When the polarity of the input plug in the DVM was switched, the absolute value was the same. Several different sets of conductivity cells were tested in a similar manner.

Figure 17 shows the cell resistance at a current of 100 nA (10^{-7} A) over a ≈30–h period at ≈400°C. An initial iR value was obtained at a current of 1 mA, which was too high and caused polarization of the specimen. At 100 nA, the ohmic value for a 4 cm^2 specimen area was ≈6.4 x 10^6 Ω, with a fluctuation of ±100 kΩ. At the end of the experiment, the specimens were raised to a position above the liquid metal, the power to the furnace was turned off, and the specimens were cooled to room temperature in flowing Ar gas.

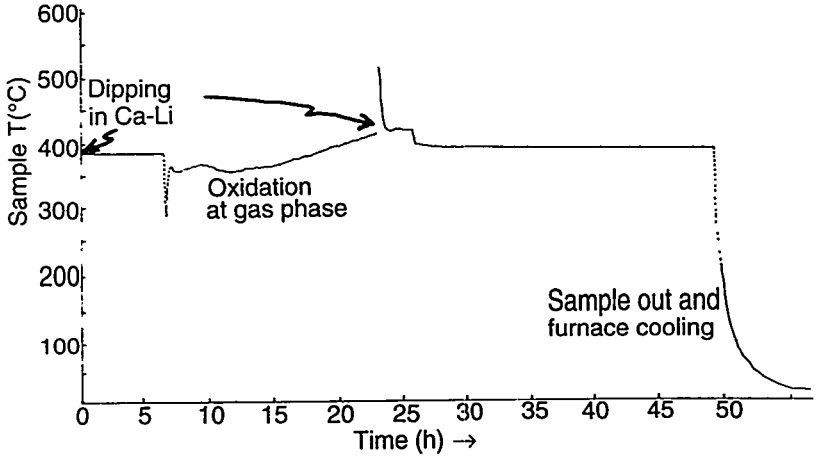

Figure 16.
Specimen temperature vs. time during CaO coating in Li containing dissolved Ca

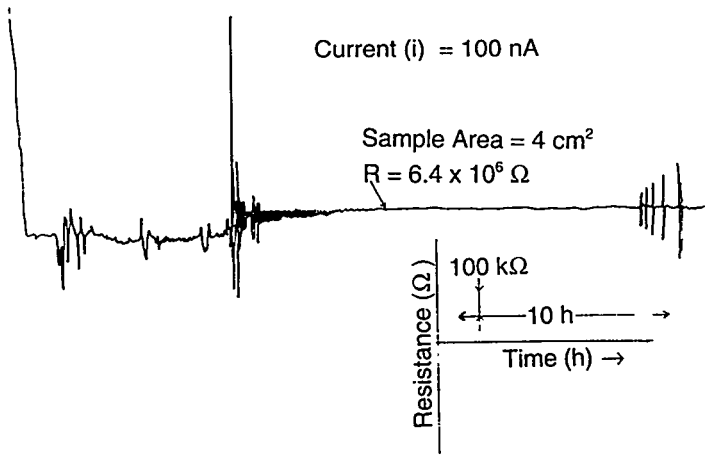

Figure 17.
Voltage (iR drop) vs. time for resistance measurements at 400°C in Li on in–situ formed CaO coating on V-5Cr-5Ti specimens

When the specimens were removed from the chamber, their surfaces were shiny due to the presence of residual liquid metal; however after a few seconds the specimens turned black because of air oxidation. The specimens were immersed in absolute alcohol to dissolve the excess metal and very soon the coating surface was revealed. A specimen was transferred to the SEM/EDS vacuum stage without total drying of the alcohol and a visual investigation of the coating surface was performed. Figure 18 (a) and (b), respectively, show an SEM photomicrograph of the surface and a topographical view that more clearly reveals surface defects. Figure 19 (a) shows another typical region of the coating surface, and 19 (b) shows a region containing microcracking of the CaO surface at high magnification.

To determine coating thickness and compositional depth profiles and to view the microcracks in cross section, the specimens were metallographically mounted using an epoxy resin. Figure 20 shows a cross section of a CaO/V-5Cr-5Ti specimen and a compositional depth profile for the CaO coating layer near the V-5Cr-5Ti interface. The photomicrograph of the CaO layer shows that cracks are perpendicular to the substrate, and that the crack tips reach the base metal. Depth profiles of the alloy elements near the interface show that the composition of Ti and Cr remain constant and that only a small amount (1-2%) of Ca diffused into the V-5Cr-5Ti (1-2 μm depth). From our previous investigation at higher temperatures (≈700°C), elemental diffusion was more significant and ≥10% V was detected in the CaO layer.[9]

Mechanical integrity and self–healing characteristics: With regard to microcracks in the coating layer, CaO has a higher coefficient of thermal expansion than that of V-5Cr-5Ti (12×10^{-6} vs. 9.2×10^{-6}/K), as shown in Fig. 21. Therefore, a CaO layer that forms in-situ on a V-alloy will be subjected to a tensile

stress during cooling. Based on the photomicrographs in Figs. 18-20, CaO coatings on V-5Cr-5Ti have the characteristics described below. The crack pattern consists of regions having a diameter of ≈30-40 μm and a crack width of ≤2000 Å over most of the CaO surface, which suggests that the cracks originate by a mismatch of the thermal expansion coefficients during cooling, i.e., "crazing cracks." Adhesion of the CaO film to the V-5Cr-5Ti substrate appears to be quite good. One approach to minimize microcracking would be to decrease the thickness of the CaO film to better match its mechanical strength with that of the V-5Cr-5Ti substrate. For example, a CaO film ≈1 μm in thickness may have a higher fracture strength and also have a resistance of ≥1 MΩ, which is higher than design requirement for ITER by 3-4 orders of magnitude. This is based on the results in Figs. 17 and 20, which indicate that a resistance of ≈6.4 MΩ for a 4 cm^2 area corresponds to a coating thickness of ≈6 μm.

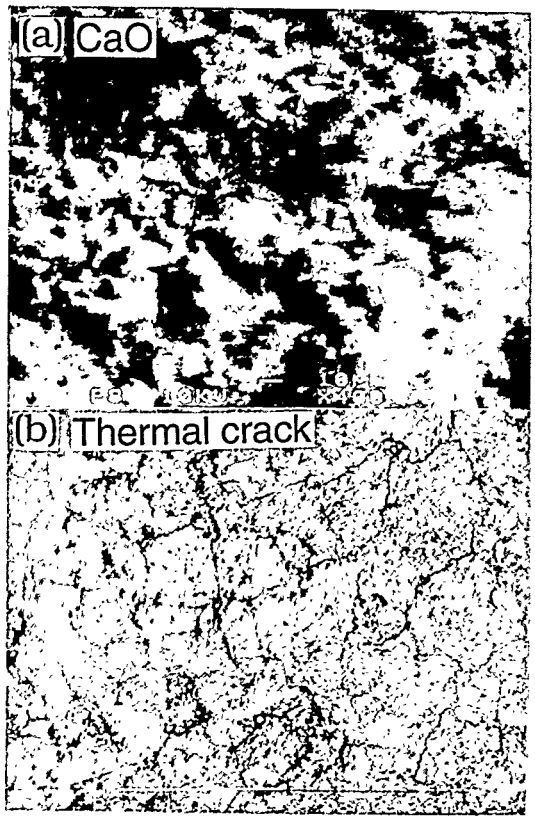

Figure 18.
(a) SEM photomicrograph of surface of CaO coating, and (b) topographical photomicrograph of (a) that reveals surface cracks

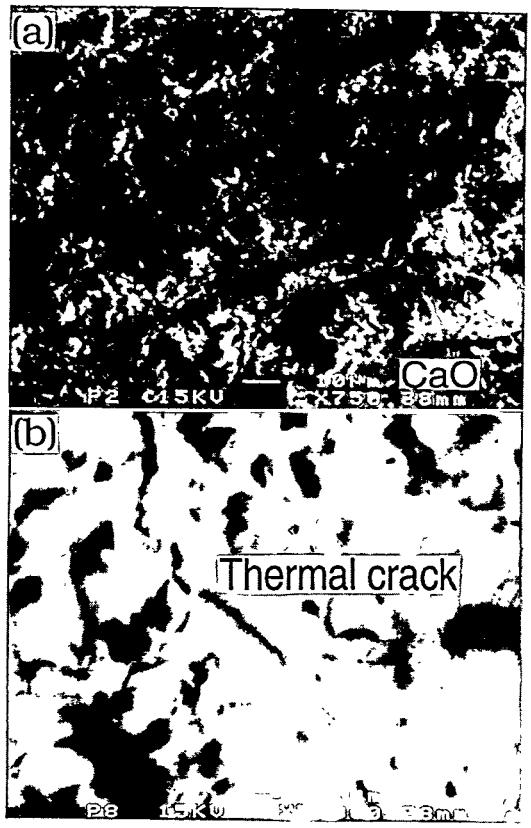

Figure 19.
(a) SEM photomicrograph of surface of CaO coating, and (b) microcracks in coating in (a) at higher magnification

Liu and Smith[10] suggest that no coating may be acceptable because calculated stresses in a coating are greater than the tensile flexural strength for most candidate coatings. Therefore, coatings are subject to cracking in both tension (e.g., CaO) and compression. However, their criterion must be viewed in relationship to the conditions under which the coating is formed (viz., temperature and time), as well as the normal operating temperature. For example, when a CaO film forms at 400°C, no stress develops when the coating operates at 400°C (Fig. 17). However, because the fabrication and operating temperatures may differ and the coating will undergo thermal fluctuation during operation, acceptable temperature ranges must be defined to account for these situations. The surface cracks shown in Figs. 18-20 developed during

cooling from 400°C to room temperature. Thermally induced strains are usually calculated by assuming linear thermal expansion, namely

$$\Delta\varepsilon_{thermal} = (\alpha_{CaO} - \alpha_{V\text{-}5Cr\text{-}5Ti}) \times (T_1 - T_2) \quad (1)$$
$$= \Delta\alpha \times \Delta T \approx 3 \times 10^{-6} \times 375$$
$$= 1.13 \times 10^{-3}$$

where α_{CaO} and $\alpha_{V\text{-}5Cr\text{-}5Ti}$ are the coefficients of thermal expansion of CaO and V-5Cr-5Ti (Fig. 21), respectively, and T_1 and T_2 are the upper and lower values of the temperature change. Stresses in the CaO coating can be relieved by either plastic deformation (including creep), crack formation (microcracking), or spallation. Plastic deformation is possible only when the stress is below the critical stress for the formation of any type of material separation (e.g., cracking).

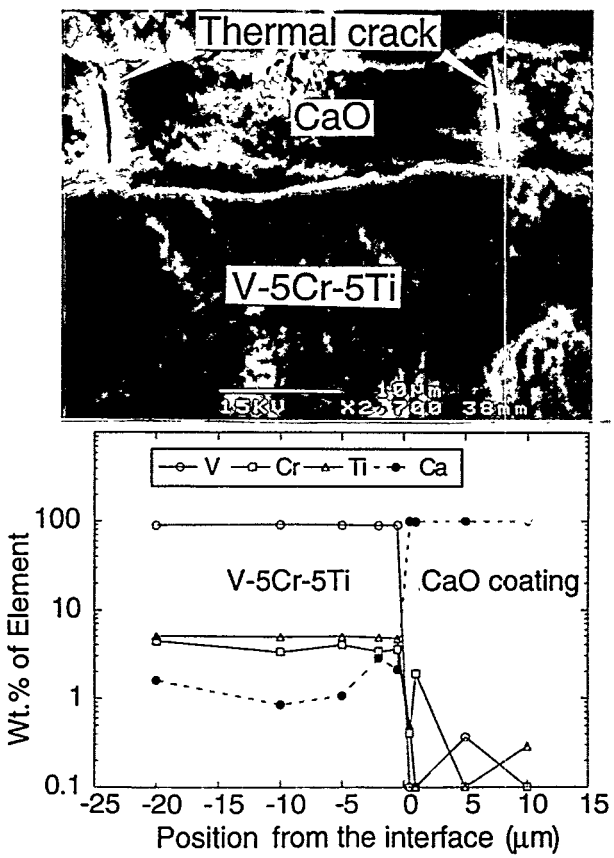

Figure 20.
SEM photomicrograph of cross section and EDS depth profiles of V, Cr, Ti, and Ca at CaO/V-5Cr-5Ti interface of a coating formed at 400°C

The CaO layer is subjected to compressive and tensile stress when the temperature is above and below that at which the film formed. When the temperature is cycled slowly, the coating/substrate interface may undergo relaxation such that cracking or spallation does not occur. In any case, cracking of the CaO layer during cooling is of most concern. Therefore, it is important for the coating to exhibit self–healing characteristics in a liquid–metal environment. Preliminary studies have been conducted to explore the self–healing properties of CaO coatings under temperature cycling. Figure 22 shows the iR response of a CaO layer on V-5Cr-5Ti during stepwise cooling in 20°C increments from 600 to 500°C. For most insulators, the ohmic value increases when temperature decreases, as shown for three increments in Fig. 22. When the temperature was decreased by ≈40°C in the last step, cracks developed and the iR value decreased suddenly but then returned to a high ohmic value indicative of self-healing behavior. This characteristic is as important as the resistivity of a coating in fusion reactor applications.

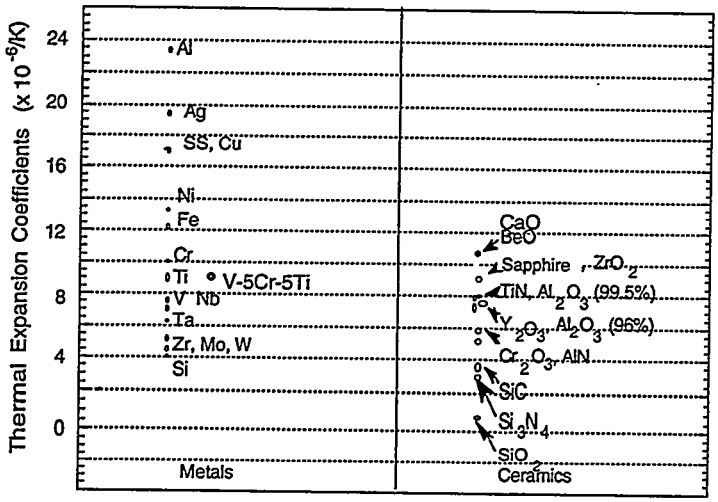

Figure 21.
Thermal expansion coefficients of various metals and ceramics

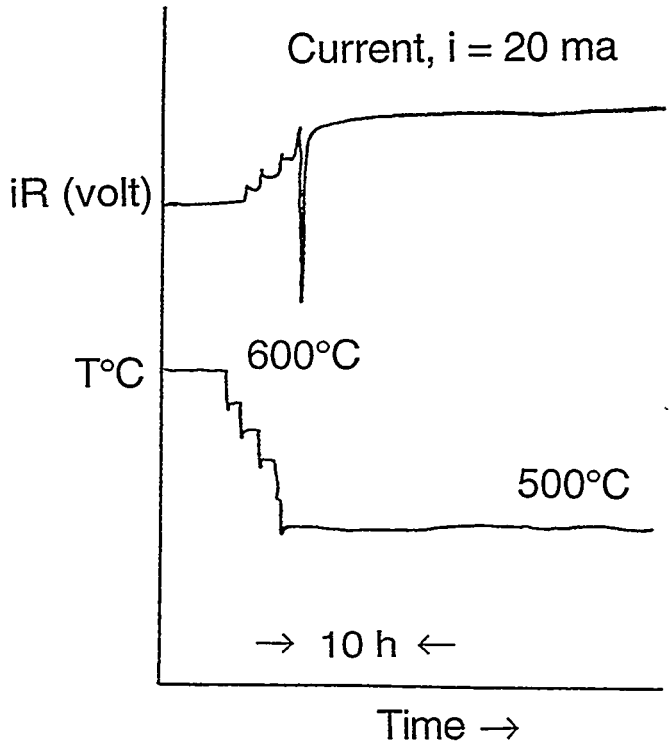

Figure 22.
Voltage (iR drop) and temperature during stepwise cooling from 600 to 500°C vs. time for resistance measurements in Li on in–situ formed CaO coating on V-5Cr-5Ti, showing an increase in resistance during small temperature decreases (20°C) and self–healing of cracks developed after larger temperature decrease (40°C) to 500°C

In other experiments, self–healing of CaO was investigated at temperatures between 300 and 740°C. At 300°C, self-healing did not occur in a 10–h period; at ≥360°C, cracks appeared to heal (e.g., at 450°C, resistivity was restored to its initial value within several hours, and at 500°C in <1 h). When a CaO coating was subjected to compressive stress by increasing the temperature in a similar manner, no appreciable cracking was detected. When temperature was increased to accelerate the healing process, we could not assess whether increases in iR values were caused by closing of cracks or by diffusion–related healing behavior. Nevertheless, when the system temperature was raised, the rapid response resembled healing of the cracks. Further work will be conducted to explore the self-healing process in terms of diffusion and thermal expansion and contraction processes within the CaO layer. With regard to self-healing, reactions that take place at the defect area (i.e., near the Li-Ca/V-5Cr-5Ti (O) interface) are of particular interest in contrast to those that occur at the CaO surface.

CONCLUSIONS AND FUTURE STUDIES

A method was developed for in-situ fabrication of a CaO electrically insulating coating on V–5Cr-5Ti in a liquid–Li environment. The process involves reaction of an O–enriched alloy surface with liquid Li containing Ca at 300–400°C. Self–healing characteristics of cracks produced in the coating by thermal cycling were also investigated. In–situ electrical resistivity measurements indicated that self–healing of defects in the coating occurred at ≥360°C. Additional work will be performed to improve mechanical stability of the coatings during thermal cycling and to establish the mechanisms for self-healing of the coatings.

ACKNOWLEDGMENTS

The author appreciate interactions with Drs. D. L. Smith and R. Mattas regarding the applicability of the work to fusion reactor designs, and with Dr. T. F. Kassner for fruitful discussions and guidance in liquid–Li-related experimental work. B. Tani of Argonne's Analytical Laboratory provided the X-ray diffraction results. R. W. Clark assisted in the liquid-lithium experiments.

REFERENCES

[1]. C. C. Baker et al., *Tokamak Power System Studies FY 1985*, Argonne National Laboratory Report ANL/FPP-85-2 (Dec. 1985).

[2]. T. Kammash, *Fusion Reactor Physics*, Chapter 15, Ann Arbor Science Pub. Inc., Ann Arbor, MI (1975), pp. 405-439.

[3]. R. F. Mattas, B. A. Loomis, and D. L. Smith, *Vanadium Alloys for Fusion Reactor Applications,* JOM, **44**(8), 26 (1992).

[4]. J.-H. Park and G. Dragel, *Development of Electrical-Insulator Coatings: In-situ Electrical Resistance Measurements on V-5%Cr-5%Ti in Liquid Lithium*, Fusion Reactor Materials Semiannual Progress Report for the Period Ending September 30, 1993, DOE/ER–0313/15, pp. 321–325 (1993).

[5]. J.-H. Park and G. Dragel, *Development of Aluminide Coatings on Vanadium–Base Alloys in Liquid Lithium*, Fusion Reactor Materials Semiannual Progress Report for the Period Ending March 31, 1993, DOE/ER–0313/14, pp. 405–410 (1993).

[6]. J.-H. Park, G. Dragel, and R. W. Clark, Development of Electrical Insulator Coatings: In-situ Electrical Resistance Measurements on CaO Coated V-5%Cr-5%Ti in Liquid Lithium, Fusion Reactor Materials Semiannual Progress Report for the Period Ending March 31, 1994, DOE/ER–0313/16, (1994).

[7]. J.-H. Park, T. Domenico, G. Dragel and R. W. Clark, Development of Electrical Insulator Coatings for Fusion Power Applications, paper submitted for 3rd Intl. Symp. on Fusion Nuclear Technology (ISFNT-3), June 27-July 1, 1994, Los Angeles, CA .

[8]. A. U. Seybolt and H. T. Sumsion, Vanadium-Oxygen Solid Solutions, J. Metals Trans. AIME, **292-299** (1953).

[9]. J.-H. Park, Intermetallic and Electrical Insulator Coatings on High-Temperature Alloys in Liquid Lithium Environments, Proc. Symp. on High-Temperature Coatings-I, TMS Fall Meeting, Oct. 2-6, 1994, Rosemont, IL

[10]. Y. Y. Liu and D. L. Smith, Ceramic Electrical Insulators for Liquid Metal Blankets, J. Nucl. Mater., **141-143**, 38 (1986).